

Ordering of a lamella-forming fluid near an interface

Andrew B. Croll, An-Chang Shi, and Kari Dalnoki-Veress*

Department of Physics and Astronomy and The Brockhouse Institute for Materials Research, McMaster University, Hamilton, Ontario, L8S 4M1 Canada

(Received 7 December 2008; revised manuscript received 15 July 2009; published 11 November 2009)

By using wedged thin films, we have measured the effect of interfaces on the ordering of an anisotropic fluid in real space. Symmetric diblock copolymers can form an ordered lamellar fluid, and the preference of the substrate for one of the blocks can induce order well into the disordered bulk phase. The induced order decays away from the substrate with a length scale that diverges at the bulk ordering transition. Ordering and disordering kinetics are found to differ: all layers relax identically upon disordering, whereas the formation of lamellae is found to vary with the distance from the substrate and can be understood from the time-dependent Ginzburg-Landau theory.

DOI: [10.1103/PhysRevE.80.051803](https://doi.org/10.1103/PhysRevE.80.051803)

PACS number(s): 83.80.Uv, 68.47.Mn, 68.55.J-, 82.35.Jk

I. INTRODUCTION

Interest in polymers at interfaces is rooted in the varied effects that have been observed, some of which are not yet fully understood. Bulk morphologies are often modified near interfaces due to finite size or confinement effects, providing an alternate route to patterning. A striking example is that of binary mixtures, where phase separation has been found to occur preferentially near an interface—*surface directed spinodal decomposition* [1]. Similarly, diblock copolymers, long chain molecules made up of segments of different chemical constituents joined together by a covalent bond, can order in the presence of an interface [2–5]. Just as a blend of two fluids can phase separate, block copolymers will also phase separate when cooled below the order-disorder transition (ODT) [7]. However, the connectivity of the two blocks restricts the separation to a molecular length scale. The details of the geometry of the resulting domains are set by the number of monomers, N , the ratio of the lengths of the two blocks, f , and the Flory-Huggins interaction parameter, χ , which specifies the incompatibility of the unlike segments and varies inversely with temperature. In the case of a symmetric diblock copolymer, $f=1/2$, and the resulting morphology is that of alternating lamellae of a -rich and b -rich domains. In the bulk, lamella will self-assemble out of the isotropic melt when $\chi N > (\chi N)_{\text{ODT}}$.

When the block copolymer melt is near a wall that has some affinity for one of the two monomers this simple description breaks down [3–6]. If the a monomers prefer the substrate, then even for temperatures, $T > T_{\text{ODT}}$, corresponding to $\chi N < (\chi N)_{\text{ODT}}$, local order is induced. An a -rich region forms near the interface, and due to the connectivity of the molecules, this forces a b -rich region to form. In analogy with surface directed spinodal decomposition [1], beyond the b -rich domain there is not an abrupt transition to a purely disordered melt but a slow screening of the surface over progressively less highly concentrated a -rich and b -rich domains. Near the ODT the system is only weakly segregated (i.e., the interface between the a and b domains is not sharp)

and we can write a decaying oscillatory concentration gradient as a function of the distance from the interface as [3–5]

$$\psi(z) \sim \exp(-z/\xi) \cos(\Omega z + \phi), \quad (1)$$

where Ω sets the period of the concentration profile and scales with the radius of gyration, R_g , of the molecule, ϕ depends on the strength of the block-interface interaction, and the concentration decays into the bulk with a characteristic length given by

$$\xi = \frac{2R_g}{\sqrt{\chi N - (\chi N)_{\text{ODT}}}}. \quad (2)$$

This analytic mean field estimate of the correlation length was predicted by Fredrickson [4], verified with the exact result from the self-consistent field theory of Shull [5], and observed with scattering [2,3] many years ago. Despite the mean field approach having some shortcomings, this analytic scaling is consistent with experimental measurements and has yet to be replaced with a more rigorous formalism.

Measurements of the concentration profile are generally inferred through fits to neutron or x-ray scattering profiles [2,3]. These types of experiments are invaluable in studying the internal structure of a material although the inherent complexity and ambiguity associated with modeling the scattering make complementary methods of great value. Here we present a simple alternative: we observe perturbations in the surface of a wedged diblock film caused by its internal concentration profile. Not only does this enable an accurate determination of ODT using only an optical microscope but we have measured the extent of the ordering induced by the substrate on an isotropic diblock melt in real space. Furthermore, we present measurements on the kinetics of ordering which reveal that the ordering and disordering kinetics differ and are well described by theory.

II. EXPERIMENT

The polymer used in this study is a monodisperse (polydispersity index of 1.09), symmetric ($f=0.50$), polystyrene-poly(2-vinyl pyridine) diblock copolymer, with a molecular weight of $M=16.5$ kg/mol, which corresponds to $N=158$

*dalnoki@mcmaster.ca

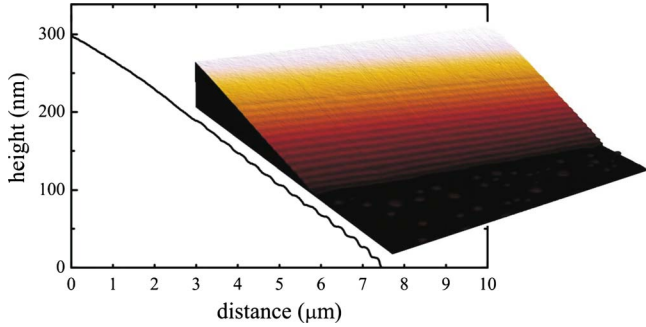


FIG. 1. (Color online) Atomic force microscopy topography image ($10 \times 10 \mu\text{m}^2$) and a height trace of a sample rapidly quenched to room temperature after equilibration at 438 K.

(Polymer Source). Samples with a gradient in the film thickness were prepared by allowing a capillary wedge to form between a silicon substrate with the native oxide layer present and a horizontal glass capillary (using a dilute polymer solution). Samples were heated using a microscope hot stage (Linkam Scientific) and observed with optical microscopy (Olympus BX51) and atomic force microscopy (AFM) (Veeco Caliber).

The films form discrete lamellar steps when ordering in order to accommodate the wedge geometry (see Fig. 1). Standard dark-field microscopy is ideal for observing the steps: light is incident on a sample at a large angle from the film normal and observations are made along the normal. As T is decreased toward T_{ODT} , ordered lamellae form and the surface of the wedged films is broken by the layer edges of the anisotropic liquid. The lamellar steps are small ($\sim 13.5 \text{ nm}$ [8]) and form ideal scattering sites, as is shown in the inset of Fig. 2. Upon cooling we observe the lamellar edges in the intensity traces of Fig. 2, which form first near the substrate (i.e., only five ordered layers are observed at 443 K), and then order sets in further into the bulk of the film as T decreases and hence ξ increases. In Fig. 2 the film is thickest on the left, i.e., order sets in on the right. We note that the magnitude of the intensity peaks does not solely reflect the degree of order but also a convolution of thin film interference effects. The scattering provided by edges and the resulting intensity profile allows for a very simple method to track the height above the substrate $L(T)$ of the highest ob-

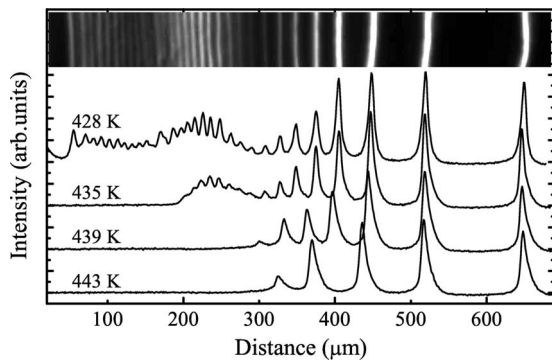


FIG. 2. A dark-field image of a wedged film at 428 K is shown in the inset. Typical intensity profiles through such images, taken at the temperatures indicated, are shown (shifted vertically for clarity).

servable ordered layer in a sample. As the temperature is changed the sample is allowed to equilibrate, the intensity profile obtained, and the number of peaks in this curve corresponds to the number of ordered layers in the sample. This methodology not only allows us to map out the equilibrium structure near ODT but also allows us to follow the dynamics of ordering in real time.

III. RESULTS

Before we analyze the ordering in detail, several qualitative observations must be made. (1) When $T > T_{\text{ODT}}$ the sample is partially ordered near the substrate and we never observe scattering at the thickest part of a wedged sample. This lack of lamellar steps is also verified with AFM measurement, which allows us to conclude that ordering is dominated by the substrate rather than air interface. This is consistent with the fact that the two blocks have very similar affinity for the air interface as the surface tensions are very similar. (2) T_{ODT} is determined to be 433 K from observation of the temperature at which a sample becomes ordered at its thickest point. (3) Measurements of the appearance or disappearance of each layer with a change in T can be made and reveal a significant difference in kinetics between disordering and ordering, with ordering being the slower process. (4) An edge appearing in the transition region from order to disorder along the gradient of the film has a lower intensity than when that same edge is fully ordered at a lower T . The latter observation suggests a relationship between the scattering intensity and the degree of order present in a sample given by the concentration envelope, $\sim \exp(-z/\xi)$, of Eq. (1). The lamellae scatter light because the edges are well defined steps, smoothed by surface tension. The intensity of light scattered from an edge correlates with the degree of ordering in a layer. This can be verified with AFM as shown in Fig. 1 for a sample equilibrated at 438 K, just above T_{ODT} . The lamellar edges become progressively less well defined as one moves away from the substrate and the concentration amplitude decreases. No ordering is observable with AFM beyond 14 layers, which corresponds exactly with the last optically observable layer at 438 K.

A. Equilibrium order near an interface

In order to analyze the data we make the following assumption: a layer edge geometry is related to the amplitude of $\psi(z)$. More precisely, the number of observable ordered layers corresponds to a depth of order into the bulk, L , which we assume to be proportional to the decay length, ξ . The number of observable ordered layers at equilibrium as a function of temperature is then a measure of the concentration profile. In Fig. 3 we plot the dimensionless length scale L/R_g , where $R_g = 3.44 \text{ nm}$ is the radius of gyration of the molecules (we have accounted for the change in lamellar spacing with T , which is $\sim 5\%$ over the entire range) [8]. The number of ordered layers diverges at $\sim 433 \text{ K}$, which corresponds to T_{ODT} , the temperature at which the entire sample orders. An alternate way to analyze the data is suggested by Eq. (2) which represents the simple analytic form suggested

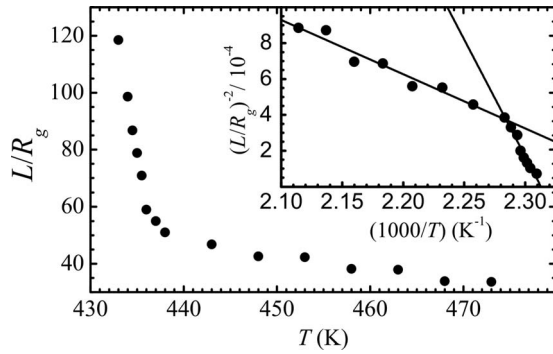


FIG. 3. Height of the topmost observable ordered lamella normalized to R_g as a function of temperature for a typical sample. The inset shows the scaling of $L(T)$ as suggested by Fredrickson [4] which reveals two linear regimes.

by Fredrickson [4] which was verified with scattering experiments [2,3]. As shown in the inset of Fig. 3, the data are indeed linear which verify that this simple approach performs as expected when compared to the more established scattering techniques. Furthermore, the data resolve the curvature observed by Menelle and co-workers [3] as two different linear regimes. To understand each region we must recognize that the two surfaces (substrate and air) compete to set the scale of the order in a sample, i.e., both induce ordering while only the substrate directed ordering is visible in our experiment. The effect of the substrate is certainly dominant as the (air) surface tension of the two components is nearly identical, i.e., the value of the concentration at the air boundary, $\psi \sim \cos(\phi_{air})$, is small relative to the substrate effect. It is then reasonable to assume that at the lowest temperatures the stronger ordering of the substrate is dominant throughout the sample, and the highest visible layer is directly proportional to the decay length, $L = k\xi$. We can directly verify this assumption for the low temperature regime: Eq. (2) and the Flory-Huggins parameter, which is typically written as $\chi = A/T + B$, result in $L^{-2} \sim A/T - A/T_{ODT}$. From the ratio of the slope to the intercept we obtain $T_{ODT} = 433 \pm 0.4$ K, consistent with the divergence of $L(T)$ in Fig. 3. When the temperature becomes higher the substrate effect damps out more rapidly and ξ decreases. Eventually, the assumption made above that the substrate amplitude dominates even at the air interface is invalid [i.e., $\exp(-h/\xi) < \cos(\phi_{air})$, with film thickness h]. Thus, the ordering at the air surface suppresses the highest observable layer since ordering at the air interface is parallel to the surface and does not form step edges which can be observed in the experiment. This transition from the substrate dominated regime to that where the air interface contributes is clearly seen in the crossover in the inset of Fig. 3.

The original mean field predictions of Leibler set the value of $(\chi N)_{ODT} = 10.495$ [9]; however, imposing the value of the spinodal point from a mean field theory that does not account for fluctuations is not reasonable [10]. We have previously measured $\chi = 97/T - 0.11$ for the identical system [8]. We consider the combination of these measurements to be an accurate and stress free determination of $(\chi N)_{ODT}$. For the system studied, $N = 158$, and we find that $\chi N_{ODT} = 18.0 \pm 1$.

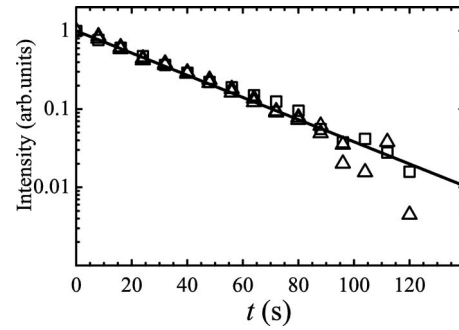


FIG. 4. The normalized intensity of light scattered from a lamellar edge as a function of time while disordering. The intensity decays as the sample is quenched from well ordered at 428 K to disordered at 435 K. Three lamellae are shown corresponding to the 19th–21st lamellae away from the substrate.

This value is reasonable since fluctuation effects drive the transition higher than Leibler's $(\chi N)_{ODT}$, though this quantity is not yet quantitatively predictable [10,11]. For example, the work of Fredrickson and Helfand suggests that $(\chi N)_{ODT}$ is increased from the mean field value of 10.495 to a value given by $(\chi N)_{ODT} = 10.495 - 41.022(Na^6v^{-2})^{-1/3}$, where the monomeric parameters a and v are the segment length and the segmental volume. A reasonable estimate of $a^3/v \sim 1$ gives $(\chi N)_{ODT} \sim 18$, which is in agreement with the measured value.

B. Dynamics of ordering

The methodology presented here provides an excellent window into ordering dynamics. The change in the intensity, I , of the scattered light from the edge of a lamellae is proportional to the change in segregation of the a and b domains, $\Delta I(T) \sim \Delta\{\exp[-z/\xi(T)]\}$. Thus, by observing the intensity of a given lamellar edge in time we gain information about the dynamics of each layer. In Fig. 4, we plot the normalized intensity, $\Delta I(t)/\Delta I$, for several lamellae as a function of time after a quench from a well-equilibrated ordered state at 428–435 K, a temperature above the ODT. One can easily identify the exponential nature of the dynamics with a time constant of $\tau = 32.8 \pm 0.4$ s. In short, as the system is quenched into the isotropic state, all the ordered lamellae disorder at the same rate and independent of the distance from the substrate, as expected since the relaxation is viscosity dominated.

In Fig. 5, we plot the intensity normalized to that of the fully ordered state for the five lamellae ranging from the 18th to the 22nd from the substrate. A disordered sample at 435 K is quenched to the ordered state at 433 K. Here we observe a significant difference from the disordering process: the intensity rises asymptotically and the process of ordering takes longer for lamellae that are further from the substrate. While qualitatively similar to bulk dynamics (see, for example, Refs. [12–18]), we emphasize that our experiments show no evidence of a traditional nucleation and growth mechanism, i.e., grains do not form and coarsen as in the bulk. The end state of a quench is the same partially ordered state described in the static experiments above. For example, layer 22 shown

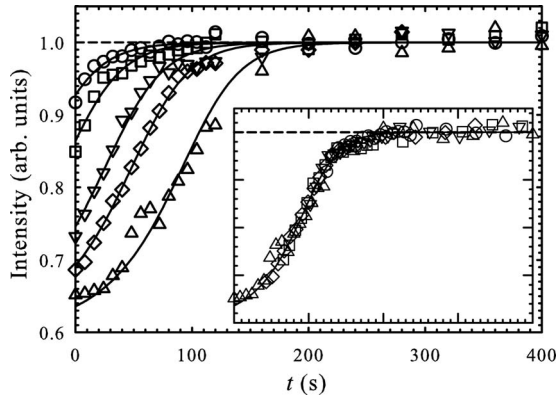


FIG. 5. The light intensity scattered from a lamellar edge as a function of time while ordering. The five lamellae are the 18th–22nd from the substrate after a quench from 435 to 433 K. The solid lines correspond to the best fit of Eq. (4), with $I_D=0.6$, $\omega=45$ s, and t_0 given in Fig. 6. The inset shows the master curve after applying the shift factors, t_0 .

in Fig. 5 is only partially ordered at the end of the quench. Layers above this height remain disordered or are ordered so weakly that they do not form layer edges. For this reason, the usual Avrami approach to the dynamics is not valid.

Despite the differences between what we observe near a surface and the bulk observations, the ordering kinetics can be understood from the time-dependent Ginzburg-Landau theory as extended to diblocks by Yamada and co-workers [19]. For a lamellar structure, the amplitude of the concentration profile, $A(t)$, evolves toward the ordered equilibrium amplitude, A_O , according to the kinetic equation,

$$\frac{dA}{dt} \sim (A_O^2 - A^2)A. \quad (3)$$

Defining $y(t)=A(t)/A_O$, the solution to this equation provides the evolution from the initial amplitude, y_0 , as $y = 1/\sqrt{1 + \exp[-2(t-t_0)]}$, with $t_0 = \ln(1/y_0^2 - 1)/2$. We emphasize that the solutions for different initial concentrations are simply shifted by the time offset t_0 . Assuming that $I \sim A$,

$$I = I_D + \frac{I_O - I_D}{\sqrt{1 + \exp[-2(t-t_0)/\omega]}}, \quad (4)$$

where I_D and I_O are the intensities measured for the fully disordered and ordered states and ω is the time constant which represents the width of the transition (note that $I_D \neq 0$ if there is a nonzero background intensity as in this experiment). The fit of Eq. (4) to the data is excellent as shown in Fig. 5, and the shift factors thus obtained can be applied to provide the master curve shown in the inset (values of t_0 shown in Fig. 6). The initial intensities follow the concentration amplitude, which is given as a function of the distance from the substrate by Eq. (1) as $y_0 = a \exp(-z/\xi)$, with $a < 1$. To first order, the plot of the shift factor, t_0 , as a

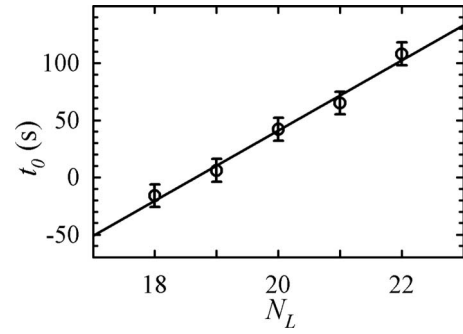


FIG. 6. Shift factors t_0 for lamellae 18–22 (see Fig. 5).

function of the distance from the substrate is linear with a slope given by $\omega/a^2\xi$. Indeed Fig. 6 is linear and the best fit line has a slope of 30 ± 2 s. With this slope, the best fit value $\omega=45$ s and taking $a \sim 0.5$, one obtains a decay length of ~ 10 which is entirely reasonable given that at 435 K, the last observable lamella is ~ 20 .

IV. CONCLUSIONS

We have presented a simple approach for the study of the effect of interfaces on the ordering of a lamella-forming fluid. The degree of order is probed with dark-field optical microscopy by light scattering from the lamellar edges at the surface of wedged diblock copolymer films. Even in the disordered state, the sample can have order induced by the presence of an interface which decays away from the perturbation. We have measured this decay in real space. With a symmetric diblock copolymer, we provide several methods of locating T_{ODT} and determine that $(\chi N)_{ODT} = 18.0 \pm 1$. The different measures of T_{ODT} show excellent agreement with each other and the concentration profile is in agreement with the scaling predicted by Fredrickson [4].

The approach presented also allows for the direct measurement of the dynamics of the ordering or disordering process of individual lamella as a function of their distance from an interface. It is found that the disordering kinetics are limited by viscous processes and are not influenced by the substrate. Experiments probing ordering show distinctly different behavior. Layers order first at the substrate and then order grows layer by layer until the profile predicted by Fredrickson is reached. This is in contrast with the bulk, where ordering proceeds by nucleation and growth. The measurements are in full agreement with the kinetics predicted by the time-dependent Ginzburg-Landau theory of Yamada and co-workers [19].

ACKNOWLEDGMENTS

The authors thank Professor Mark Matsen for valuable discussions. Financial support from NSERC and the ACS PRF is gratefully acknowledged.

- [1] R. A. L. Jones, L. J. Norton, E. J. Kramer, F. S. Bates, and P. Wiltzius, *Phys. Rev. Lett.* **66**, 1326 (1991).
- [2] M. D. Foster, M. Sikka, N. Singh, F. S. Bates, S. K. Satija, and C. F. Majkrzak, *J. Chem. Phys.* **96**, 8605 (1992).
- [3] A. Menelle, T. P. Russell, S. H. Anastasiadis, S. K. Satija, and C. F. Majkrzak, *Phys. Rev. Lett.* **68**, 67 (1992).
- [4] G. H. Fredrickson, *Macromolecules* **20**, 2535 (1987).
- [5] K. R. Shull, *Macromolecules* **25**, 2122 (1992).
- [6] H. Tan, D. Yan, and A.-C. Shi, *Macromolecules* **37**, 9646 (2004).
- [7] G. H. Fredrickson and F. S. Bates, *Annu. Rev. Mater. Sci.* **26**, 501 (1996).
- [8] A. B. Croll, M. W. Matsen, A.-C. Shi, and K. Dalnoki-Veress, *Eur. Phys. J. E* **27**, 407 (2008).
- [9] L. Leibler, *Macromolecules* **13**, 1602 (1980).
- [10] G. H. Fredrickson and E. Helfand, *J. Chem. Phys.* **87**, 697 (1987).
- [11] O. Vassiliev and M. W. Matsen, *J. Chem. Phys.* **118**, 7700 (2003).
- [12] J. H. Rosedale and F. S. Bates, *Macromolecules* **23**, 2329 (1990).
- [13] G. H. Fredrickson and K. Binder, *J. Chem. Phys.* **91**, 7265 (1989).
- [14] T. Hashimoto and N. Sakamoto, *Macromolecules* **28**, 4779 (1995).
- [15] J. D. Wilbur, Z. Fang, B. A. Garetz, M. C. Newstein, and N. P. Balsara, *Macromolecules* **41**, 4464 (2008).
- [16] T. Hashimoto, K. Kowsaka, M. Shibayama, and H. Kawai, *Macromolecules* **19**, 754 (1986).
- [17] M. A. Singh, C. R. Harkless, S. E. Nagler, R. F. Shannon, and S. S. Ghosh, *Phys. Rev. B* **47**, 8425 (1993).
- [18] S. H. Anastasiadis, *Curr. Opin. Colloid Interface Sci.* **5**, 324 (2000).
- [19] K. Yamada, M. Nonomura, and T. Ohta, *Macromolecules* **37**, 5762 (2004).